

AN ABSTRACT OF THE THESIS OF

Paula Sonawala for the degree of Master of Science in Physics

presented on June 1, 1988.

Title: Rotation of polarization in single mode fibers and its relation
to Berry's phase

Redacted for privacy

Abstract approved: _____

Clifford Fairchild

The polarization state of light in a single mode optical fiber may be changed by linear and circular birefringence intrinsic to the fiber or introduced by stress in the fiber due to external pressure, bends or twists. Rotation of polarization may also occur in the absence of any intrinsic or stress induced birefringence, if the fiber is bent into a nonplanar curve. Such rotation depends purely on the path of the fiber and is therefore known as geometric or topological rotation of polarization.

An experiment was carried out to measure this geometric rotation of polarization by laying the fiber in different helical paths. Measurements of polarization rotation were made for each of twelve different fiber helices. A personal computer was used for experimental control and data acquisition.

The theory of the geometric rotation of polarization can be explained using classical electrodynamics, and an independent quantum mechanical treatment based on Berry's topological phase. Both theories are discussed in this work. The experimental results were compared with both theories and agreement with both was obtained.

ROTATION OF POLARIZATION IN SINGLE MODE OPTICAL
FIBERS AND ITS RELATION TO BERRY'S PHASE

BY

PAULA SONAWALA

A THESIS

submitted to

OREGON STATE UNIVERSITY

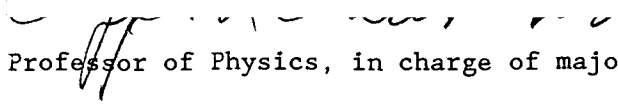
in partial fulfillment of
the requirements for the
degree of
MASTER OF SCIENCE

Completed on June 1, 1988

Commencement June, 1989

APPROVED:

¹
Redacted for privacy



Professor of Physics, in charge of major

Redacted for privacy

Head of department, Physics

Redacted for privacy

Dean of Graduate School

Date thesis is presented June 1, 1988

Typed by Paula Sonawala for Paula Sonawala

ACKNOWLEDGEMENTS

This work is dedicated to my family, who have always inspired and encouraged me in all my endeavours.

I am grateful to my adviser, Dr. Fairchild, for his valuable advice and enthusiastic support. A special thanks to Juergen Anders for his assistance in this project and many helpful suggestions.

I would like to thank Dr. Krane for his guidance and support throughout my stay at Oregon State.

And to the friendly staff of the Physics Department, a very special thanks for their assistance in typing the thesis.

TABLE OF CONTENTS

CHAPTER 1. INTRODUCTION	1
1.1 What is an optical fiber?	2
1.2 Propagation modes inside an optical fiber	6
1.3 Wave equations inside an optical fiber	7
CHAPTER 2. POLARIZATION PROPERTIES OF A SINGLE MODE FIBER	11
2.1 An overview of birefringence in optical systems	11
2.2 Propagation of polarization in single mode fibers	17
2.3 Birefringence in single mode fibers	19
CHAPTER 3. GEOMETRIC ROTATION OF POLARIZATION	22
3.1 Propagation of polarization in a curved fiber	23
3.2 Origin of the geometric rotation	24
3.3 Mathematical derivation for the geometric rotation in a helical fiber	27
CHAPTER 4. BERRY'S TOPOLOGICAL PHASE	30
4.1 General derivation of Berry's phase	31
4.2 Properties and significance of Berry's phase	34
4.3 Manifestation of Berry's phase in physical system	36
CHAPTER 5. AN EXPERIMENT TO MEASURE THE GEOMETRIC ROTATION OF POLARIZATION IN LOW BIREFRINGENCE SINGLE MODE FIBERS	40
5.1 Experimental setup	40

5.2 Theoretical calculation of the rotation	45
5.3 Data analysis	49
5.4 Error analysis	56
5.5 Extension of the experiment to measure Faraday rotation	58
CHAPTER 6. SUMMARY AND CONCLUSIONS	60
REFERENCES	62

LIST OF FIGURES

<u>FIGURE</u>	<u>PAGE</u>
1.1a. A typical optical fiber	3
1.1b. Typical fiber geometries	3
1.2. Light propagation in an optical fiber	4
1.3a. Structure and refractive index of a step index fiber	5
1.3b. Structure and refractive index of a graded index fiber	5
1.4. Low order modes of an optical fiber	10
2.1a. Linear birefringence in a half wave plate	13
2.1b. Circular birefringence	14
2.2. Phase shifts for the parallel and perpendicular components of the E field for internal reflections	18
3.1. Geometric rotation of polarization	26
3.2. Axes used to describe the polarization state in a fiber	28
5.1. Schematic of the experimental setup	41
5.2. A sample intensity plot	46
5.3a. Helix geometry	48
5.4(a-d). Plots of measured rotation of polarization in a single mode optical fiber	52

LIST OF TABLES

<u>TABLE</u>	<u>PAGE</u>
5.3. Measured and calculated values of rotation for different cylinders and deformations.	51
5.4. Beat lengths of induced birefringence for different cylinders.	51

ROTATION OF POLARIZATION IN SINGLE MODE OPTICAL FIBERS
AND ITS RELATION TO BERRY'S PHASE

CHAPTER 1

INTRODUCTION

The silica glass fiber or the optical fiber, as it is popularly known, has truly revolutionised the communication technology today. The combination of low loss and wide bandwidth available at optical frequencies make these fibers extremely attractive for use as a transmission medium in telecommunication systems. Also, whereas the metallic transmission lines suffer from exponentially increasing conducting losses at higher frequencies, the losses of fibers are far less, there-by allowing repeaters to be spaced further apart.

Much of the research and development in the area of integrated optics has also been stimulated by technological breakthroughs in the understanding and production of low loss fibers.

Further advances in fiber optics technology has enhanced their scope of application from the traditional realm of telecommunication. Fibers are extensively used today as various kinds of sensors such as remote light sensors, pressure sensors, interferometric sensors, polarization sensors and even optical gyroscopes.

It is thus essential to study and understand the different properties of the fiber, like transmission loss, polarization and birefringence, etc., for effective application of these fibers.

1.1 WHAT IS AN OPTICAL FIBER ?

An optical fiber is essentially a dielectric waveguide. A typical optical fiber, shown in fig.1.1(a) is a cylindrical structure, consisting of a central core of radius a and index of refraction n_2 surrounded by a concentric cladding of a slightly lower refractive index n_1 . Typical fiber geometries are shown in fig.1.1(b)¹⁻³.

Confined and lossless propagation in fibers is accomplished by total internal reflection from the dielectric interface between the core and the cladding. This requires the refractive index of the core to be greater than the cladding. It also requires that the angle of incidence of the core be greater than the critical angle.

$$\text{i.e. } \theta_i > \theta_c = \sin^{-1}(n_1/n_2)$$

This is shown schematically in fig.1.2.

The light then propagates inside the fiber by successive internal reflections. This is the basic principle of light propagation in an optical fiber.

According to the refractive index profile of the core and the cladding, the fibers are classified as step index or graded index fibers. The geometries of the step index and graded index fibers are shown in fig.1.3(a), (b).

A step index fiber consists of a core of refractive index n_1 and radius a , and a cladding of refractive index n_2 and a radius b . The radius b of the cladding is chosen large enough so that the field of

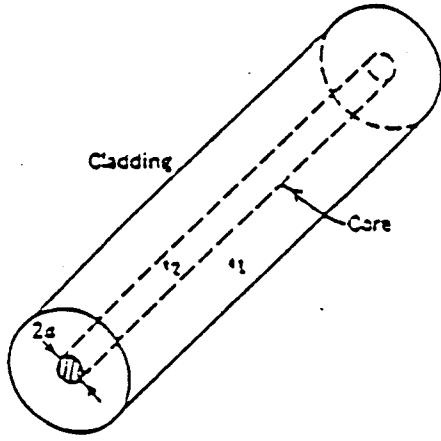


Fig. 1.1a A typical optical fiber

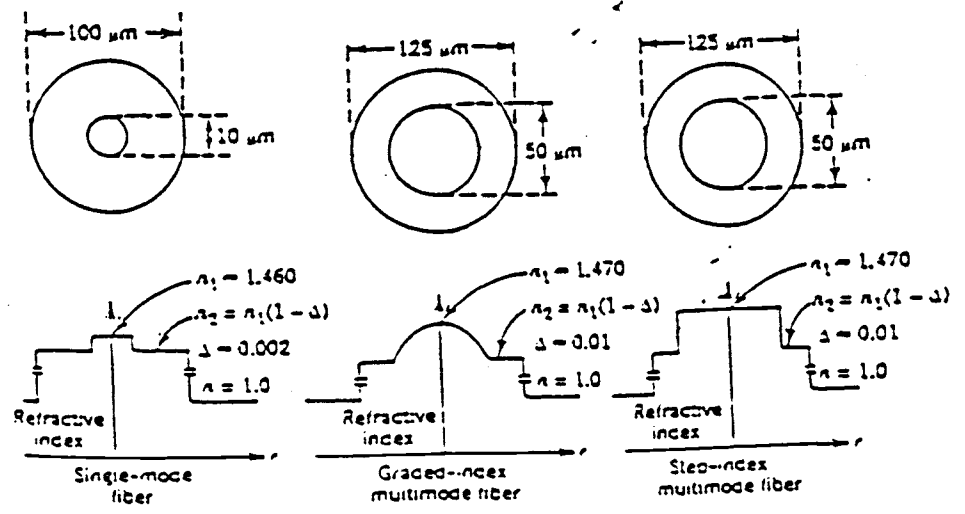


Fig. 1.1b Typical fiber geometries

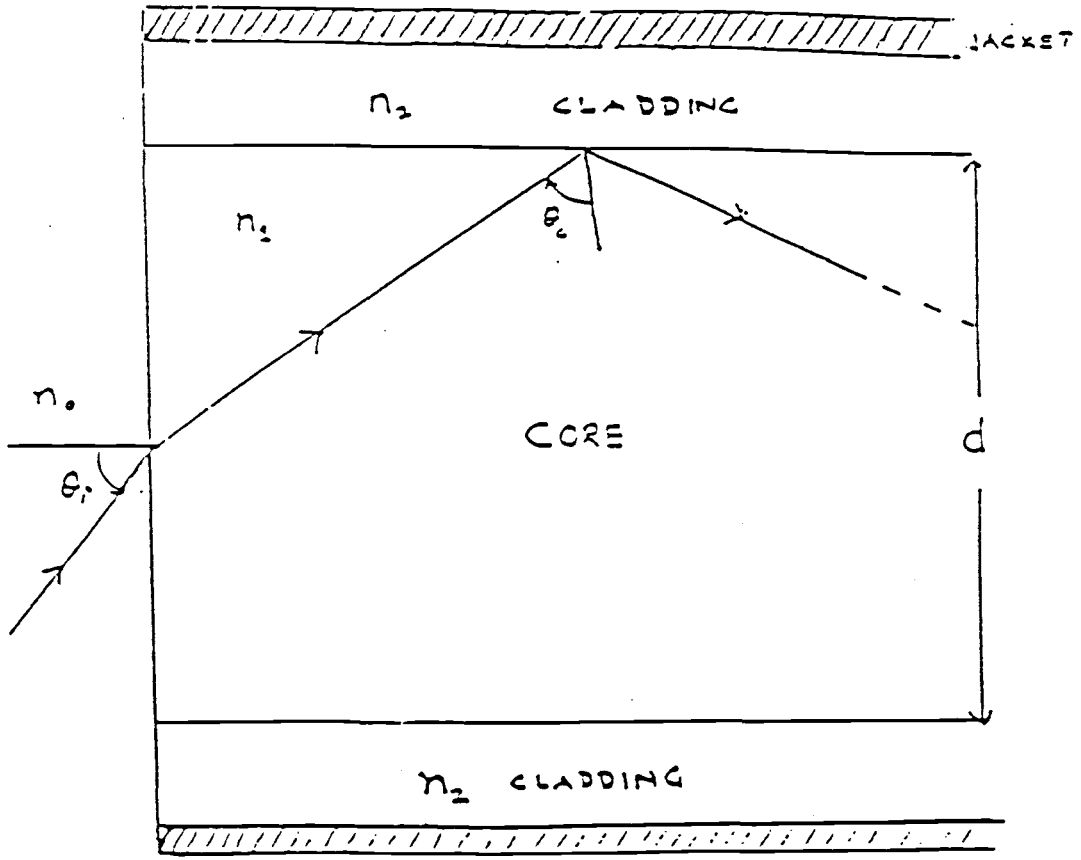


Fig 1.2 Light propagation in an optical fiber

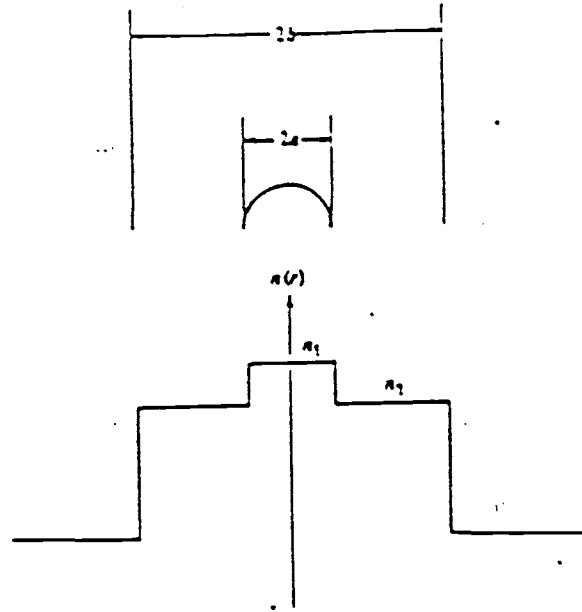


FIG. 1.3a. Structure and refractive index of a step index fiber

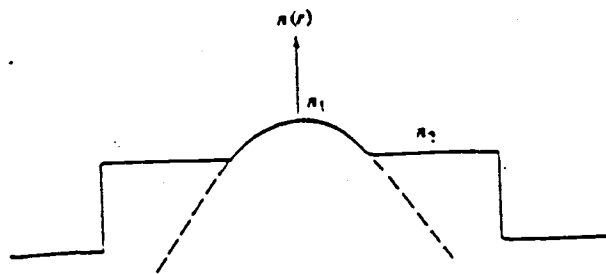


FIG. 1.3b. Structure and refractive index of a graded index fiber

confined modes is virtually zero at $r = b$.

A graded index fiber differs from a step index fiber in that the index of refraction is a continuous variable function of the radial distance from the fiber axis. In the simplest configuration, the index is maximum on the axis, decreases with r , for $r < a$ and is constant for $r > a$. Also, the manner in which a graded index fiber guides the fiber is not reflection at a dielectric discontinuity, but by continuous bending of the propagation vector k , as it moves through the region of continuously changing index of refraction.

Graded index fibers are becoming increasingly important in fiber optics communication today, because they offer a multimode propagation in a large core fiber coupled with low modal birefringence. The analysis of fields inside a graded index fiber is more complicated than the step index fiber. We will mainly limit our discussion to propagation inside step index fibers.

1.2 PROPAGATION MODES INSIDE A FIBER

The electric and magnetic fields of the light propagating inside a planar dielectric can be resolved into a z -component parallel to the waveguide axis and its x -component normal to the axis. Propagation is possible only when the x components form standing waves since only these can interfere constructively. As a result, only a finite number of modes are allowed to propagate. These are called transverse modes and are labelled TE or TM depending on whether the E or the B field is

transverse to the waveguide axis. A fiber can thus have one or more modes travelling in it. A fiber designed to propagate only one mode is called a single mode fiber. Single mode fibers have lower modal dispersion than multimode fibers. They also have better polarization preserving properties. But, the numerical aperture of a single mode fiber is much smaller and coupling light into the fiber is more difficult. However, single mode fibers are finding a wide range of applications in communication systems and fiber optic sensors.

The condition for a fiber to be single mode can be derived accurately by solving the wave equation inside the fiber. This is discussed in the following section.

1.3 WAVE EQUATIONS INSIDE AN OPTICAL FIBER

The ray picture of light propagation through a fiber, is only an approximation for fibers with dimensions much larger than the wavelength of light. Particularly, for single mode fibers, where the core diameter is comparable to the wavelength of light, it is necessary to use wave optics to get a more accurate description of light propagation. To derive the exact wave equations in the fiber we need to solve Maxwell's equations with appropriate boundary conditions. The exact solutions of such a cylindrical step index dielectric waveguide are very complicated and involve hybrid EH_{1m} and HM_{1m} modes which have six nonzero field components, rather than the simple TE and TM modes.

A good approximation of the field components and mode conditions

can be obtained in most fibers whose core refractive index is only slightly higher than the cladding medium, i.e. $(n_2 - n_1 \ll 1)$. In this approximation, the continuity conditions at the core cladding interface are simplified, thus allowing us to use Cartesian field components as above. Fibers that satisfy this condition are called weakly guiding fibers.

In this approximation, we can write the wave equation inside the fiber as :

$$[\partial^2/\partial r^2 + (1/r)\partial/\partial r + (1/r^2)\partial^2/\partial \phi^2 + (k^2 n_j^2 - \beta^2)]\psi_z \quad (1.1)$$

where n_j is n_1 for the core and n_2 for the cladding.

ψ_z corresponds to the z component of the electric or the magnetic field inside the fiber.

The solution of 1.1 is assumed to be of the form:

$$E(r, \phi, z, t) = E(r, \phi) \exp[i(\omega t - \beta z)] \quad (1.2)$$

where $\omega = ck$ is the frequency in radians and β , the longitudinal propagation constant of the wave. It can be seen from the form of eqn. 1.1, that the field variation along r will depend on the value of $(k^2 n_j^2 - \beta^2)$ and will be sinusoidal for $(k^2 n_j^2 - \beta^2) > 0$ and exponential for $(k^2 n_j^2 - \beta^2) < 0$. Modes having physical significance can exist only with propagation constants smaller than kn_1 , else they will be evanescent everywhere. On the other hand, propagation constants smaller than kn_2 correspond to fields that oscillate everywhere and thus do not vanish at $r \rightarrow \infty$. Thus, we have the condition,³

$$kn_2 \leq \beta \leq kn_1$$

For a fiber with radius a , we define the parameters

$$u = a \sqrt{k^2 n_{\text{core}}^2 - \beta^2}$$

$$v = a \sqrt{\kappa^2 n_{\text{cladding}}^2 - \beta^2}$$

Then, substitution of 2 into 1 gives $E(r, \phi)$ in terms of Bessel functions as $J(ur/a)$ and $K(vr/a)$.

We can define a third parameter

$$V = u^2 - v^2 = a^2 k^2 (n_{\text{core}}^2 - n_{\text{cl}}^2)$$

This is called the normalized frequency. Fig.1.3 shows the low order modes propagating in a fiber and their propagation constants as a function of V . It can be seen that in order to get a single mode, $V < 2.405$.

The exact solutions of the wave equation, HE_{1m} modes can be replaced by linearly polarized LP_{1m} modes in the weakly guided fibers. The subscripts l and m give the number of azimuthal and radial modes, respectively. The fundamental LP_{01} mode therefore does not have an azimuthal component and has a circular beam shape. In fact, the field distribution of the fundamental mode is approximated to be a gaussian distribution. This is also the beam characteristic of a single mode fiber.

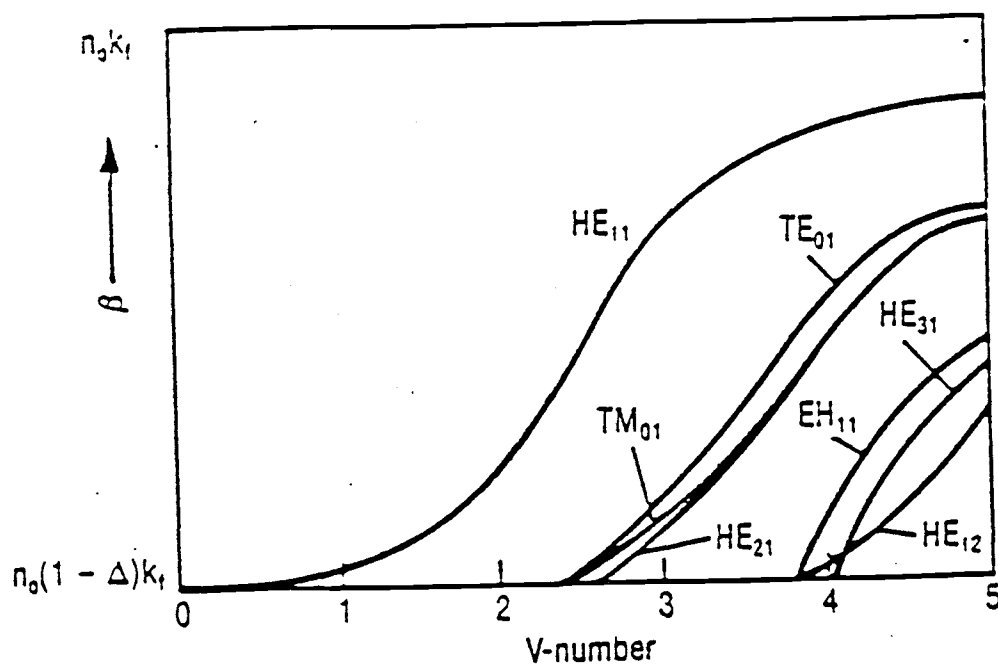


FIG 1.4.

Low order modes of an optical fiber

CHAPTER 2

POLARIZATION PROPERTIES OF A SINGLE MODE FIBER

In applications of single mode fibers as polarimetric devices like current sensors, rotation sensors, optical gyroscopes and other interferometric devices, the fiber operates with coherent polarized light. So a thorough understanding of their polarization properties is important for successful construction and operation of such devices.

2.1 AN OVERVIEW OF BIREFRINGENCE IN OPTICAL SYSTEMS

A material which displays two indices of refraction in two different directions is called a birefringent substance and the phenomenon is called birefringence. The origin of birefringence lies in the structural anisotropy of the material. This results in optical anisotropy, i.e. the optical properties of the material are not all the same in all directions.

There exists, however, one direction of propagation in the crystal which does not exhibit this optical anisotropy and is called the optical axis of the material. The refractive indices for directions perpendicular (n_{\perp}) to and parallel (n_{\parallel}) to this direction are different. This difference ($n_{\perp} - n_{\parallel}$) is a measure of the birefringence of the material.

LINEAR BIREFRINGENCE: Now consider linearly polarized light propagating in the direction of the optical axis inside such a material. The parallel and perpendicular components of the E field then travel with different propagation constants, resulting in a phase lag between the two components. Thus the resulting wave will be elliptically polarized in general. This phenomenon is called linear birefringence and is illustrated in fig.2.1a for a half wave plate.

OPTICAL ACTIVITY OR CIRCULAR BIREFRINGENCE: The phenomenon, whereby the plane of polarization of linear light undergoes a rotation as it propagates through a material is called optical activity or circular birefringence.

A material which exhibits optical activity is called an active material. Such a material has different refractive indices for the left and right circularly polarized light i.e. n_l and n_r .

Now, linearly polarized light can always be represented as a superposition of left and right circularly polarized light. Each of the two components propagate with different propagation constants in the medium. Thus, in traversing the medium, the two get out of phase, and the resultant linear wave appears to have rotated. This is illustrated in fig.2.1b.

2.1.2 JONES MATRICES

A compact and elegant representation of polarized light was invented by American physicist R.K.Jones. In this formalism, a polarized light wave is represented in terms of the electric field.

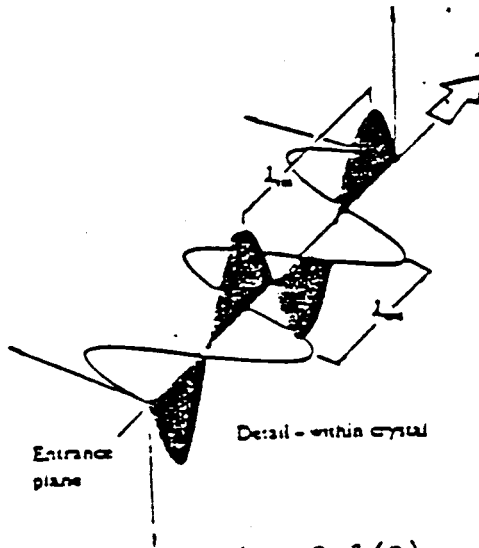
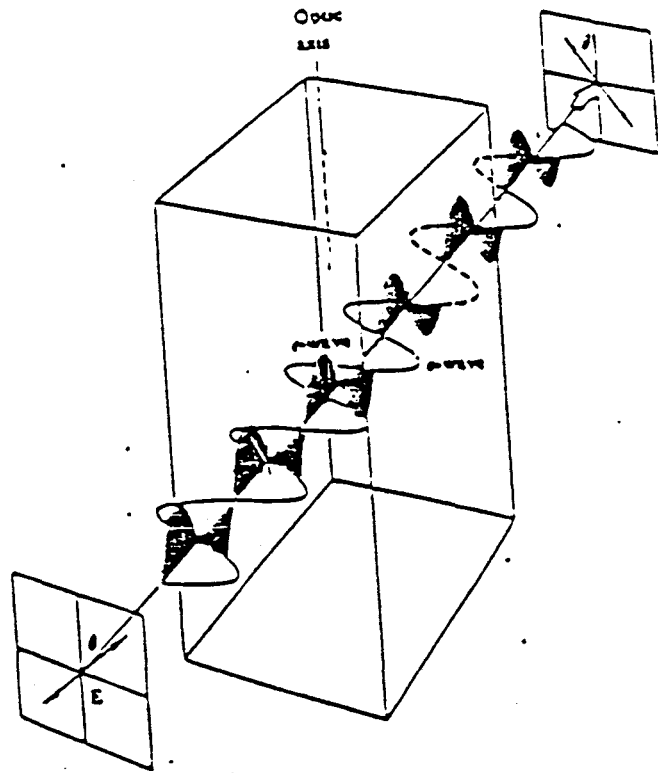


Fig. 2.1(a).

Linear birefringence in a half wave plate

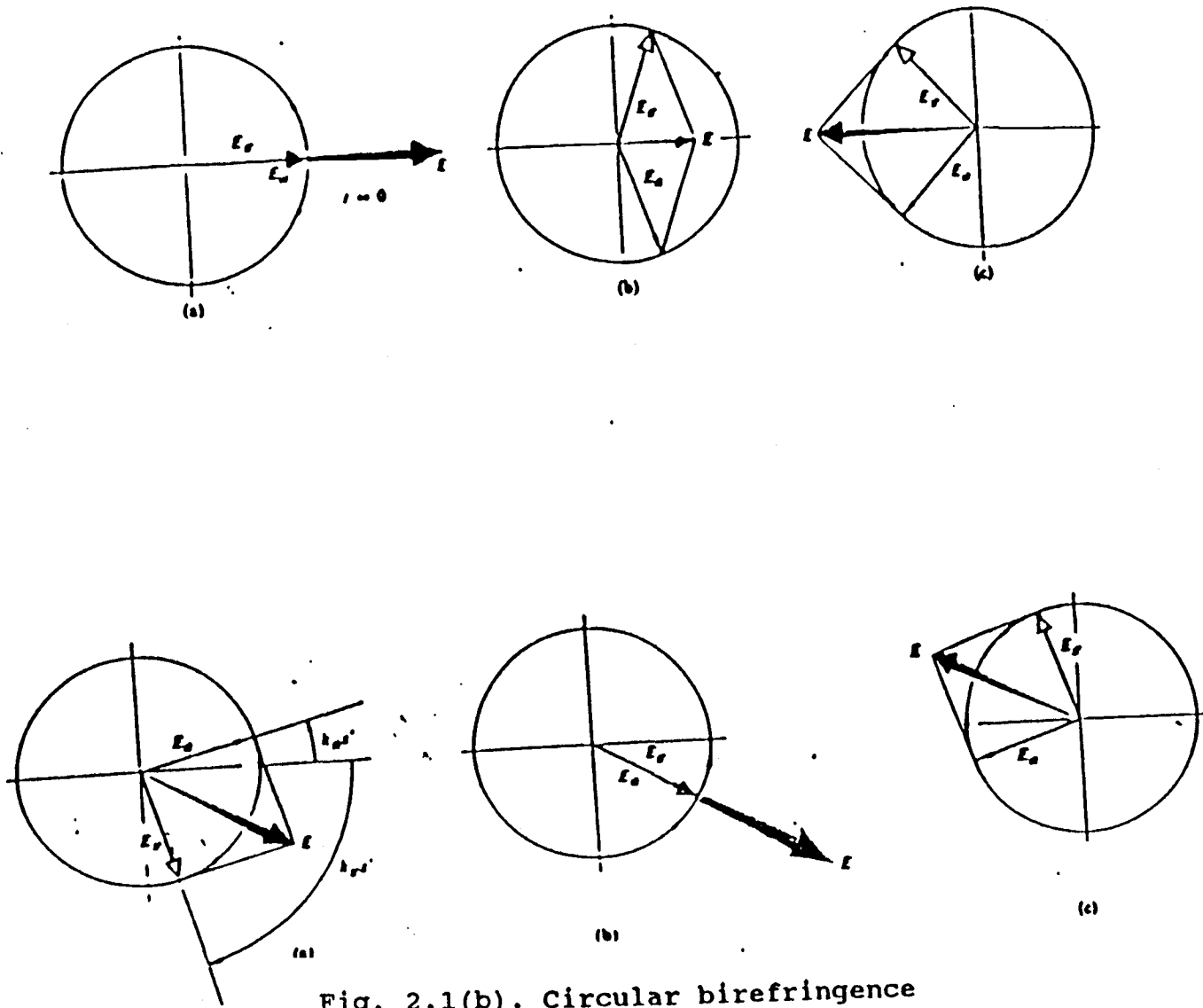


Fig. 2.1(b). Circular birefringence

$$E = \begin{bmatrix} E_x(t) \\ E_y(t) \end{bmatrix} \quad (2.1)$$

$E_x(t)$ and $E_y(t)$ are the instantaneous scalar components of E . Obviously, knowing E , we know everything about the polarization state. We can deal with coherent waves, if the phase information is also preserved. We then write eqn. 2.1 as

$$E = \begin{bmatrix} E_x \exp(i\phi_x) \\ E_y \exp(i\phi_y) \end{bmatrix} \quad (2.2)$$

Now, suppose that we have a polarized incident beam represented by this Jones's vector E_i , which passes through an optical element, emerging as a new vector, E_t . This can be described mathematically using a 2 2 matrix. Let the transformation be represented by a matrix S , where

$$S = \begin{bmatrix} a_{11} & a_{12} \\ a_{21} & a_{22} \end{bmatrix} \quad (2.3)$$

The four matrix elements are complex, in general, and contain a complete description of the birefringence properties of the optical system.

The emerging light can then be described as:

$$E_t = SE_i \quad (2.4)$$

If the wave passes through a series of optical elements represented by

the matrices $S_1, S_2, \text{ etc.}$, then

$$E_t = S_n \dots S_1 E_1 \quad (2.5)$$

Note that these matrices do not commute and must be applied in the proper order.

The Jones's matrix, for light propagating along the optical axis of a system with linear birefringence is given as⁸⁾:

$$S = \begin{bmatrix} \exp(i\delta_1/2) & 0 \\ 0 & \exp(-i\delta_1/2) \end{bmatrix} \quad (2.6)$$

where δ_1 = measure of the linear birefringence

Since the effect of the linear birefringence is to introduce a phase retardation between the two components of the E field, this term appears as an exponential in the matrix.

For example, consider an optical system like a quarter wave plate.

The effect of such an element is to convert linearly polarized light to circularly polarized light by introducing a phase lag of $\pi/2$ between the two components of the linear light. So, the Jones matrix for a quarter wave plate is

$$S = \begin{bmatrix} \exp(i\pi/4) & 0 \\ 0 & -i\exp(i\pi/4) \end{bmatrix} \quad (2.7)$$

For a system with circular birefringence

$$S = \begin{bmatrix} \cos(\delta_c/2) & \sin(\delta_c/2) \\ -\sin(\delta_c/2) & \cos(\delta_c/2) \end{bmatrix}$$

where δ_c = measure of the circular birefringence.

This is simply a rotation matrix so that for the transmitted light, the plane of polarization rotates by an angle = $\delta_c/2$.

2. 2 PROPAGATION OF POLARIZATION IN SINGLE MODE FIBERS

As discussed in Chapter 1, the propagation of polarization in an optical fiber is by the phenomena of total internal reflections. When light is internally reflected, the perpendicular and parallel components of the E field undergo different phase shifts, as indicated by fig. 2.2. If LPL is launched inside a straight fiber such that the E field is polarized perpendicular to the waveguide axis, then there is no parallel component of the E field at any time and hence in the absence of any birefringence, the polarization state of LPL is preserved. Further, in the case of weakly guided fibers, the difference between the refractive indices of the core and the cladding is considered to be negligible, i.e. $(n_2 - n_1) \ll 1$. In this approximation, the internal angle is always taken to be close to 90° , so that there is no phase shift between the parallel and perpendicular components of the E field propagating inside the fiber, even if it is not polarized perpendicular to the waveguide axis, in the case of such weakly guiding fibers.

So, in general, we assume that an ideal fiber with no intrinsic or stress induced birefringence, preserves the state of polarization. As we will see in the next section, this is not always true.

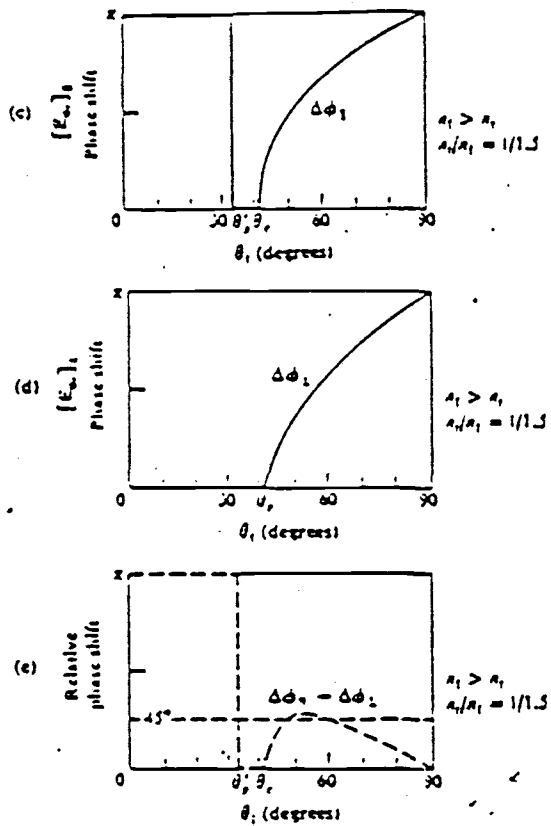


Fig.2.2

Phase shifts of the parallel and perpendicular components of the E - field for internal reflections

2.3 BIREFRINGENCE IN SINGLE MODE OPTICAL FIBERS

An ideal optical fiber is assumed to be perfectly cylindrical with a circularly symmetric refractive index distribution. This leads to perfect degeneracy of the two linearly polarized modes, i.e. the x and y linearly polarized modes with the same propagation constants.

However, actual fibers exhibit some ellipticity of the core and some anisotropy in the refractive index distribution which arises due to the presence of anisotropic stresses. In the presence of anisotropic stresses, the dielectric permittivity is no longer a scalar, but is a tensor. This results in two different propagation constants for the x and y polarized modes, leading to perturbations of the state of polarization of the light transmitted by the fiber. The difference in the propagation constants is defined as birefringence(β)³.

The practical parameter used to study the polarization preserving properties of an optical fiber is the beat length, defined as

$$L = 2\pi/\beta$$

where β is the birefringence.

Optical fibers with beat lengths longer than one meter are commercially called low birefringence fibers. Beat length measurements have been made in the past by using techniques such as:⁹⁾

- 1). Optical polarization
- 2). Rayleigh Scattering
- 3). Electro-optic modulation

- 4). Wavelength Sweeping
- 5). Polarization dispersion
- 6). Application of lateral stress
- 7). Optical Heterodyne interferometry

Anisotropic stresses could be present in the fiber because of built-in anisotropies resulting from the fabrication process or could be induced externally. The resulting birefringence effects are called intrinsic or induced birefringence effects.

2.3.1 INTRINSIC BIREFRINGENCE

Intrinsic birefringence is that present in the fiber due to built in anisotropies resulting from the fabrication process. If the core is not circular but elliptic, then the x and y polarized modes will have different propagation constants resulting in linear birefringence. This is called shape induced birefringence.

Because the materials used to manufacture optical fibers have different thermal coefficients, it is possible to build anisotropies in the fiber due to photoelastic effect. For good quality fibers this corresponds to a very low birefringence or a very long beat length.

2.3.2 INDUCED BIREFRINGENCE

1. BEND INDUCED BIREFRINGENCE

When a fiber of outer radius r is bent along a curve of radius R ($R \gg r$) then the induced linear birefringence is given by:

$$\beta_b = \Gamma r^2 k$$

where k = curvature of the bend

Γ = a constant ≈ 0.093 for 633nm

Again, this results because of the stress induced due to bending.

2. TWIST INDUCED BIREFRINGENCE

Twisting a fiber with a uniform twist rate $2\pi N$ (rad/m) where N is the number of turns per meter, will induce a shear stress that leads to circular birefringence in contrast to other stress induced effects.

Thus the state of polarization of linearly polarized light is preserved but it is rotated by an angle θ .

The induced birefringence is given by³⁾:

$$\beta_t = g\tau$$

where τ = twist rate = $2\pi N$, for N turns

and g = constant = -0.16

3. EXTERNAL FIELDS: FARADAY ROTATION

A magnetic field applied longitudinally along the fiber axis will induce a circular birefringence through the Faraday Effect. The rotation is given by

$$\theta_F = V \oint \vec{H} d\vec{l}$$

Where H is the magnetic field and

V is the Verdet's constant of the material

If the magnetic field is produced by a current I flowing through N turns of a coil, then, using Ampere's Law, we can write the rotation as

$$\theta_F = VNI$$

Thus the rotation of polarization is a measure of the current.

CHAPT. 3

GEOMETRIC ROTATION OF POLARIZATION

The polarization of light propagating in a single mode fiber can also be rotated in the absence of any natural birefringence or stress induced effects if the fiber is bent into a nonplanar curve. Such a rotation depends only on the geometry of the path of the fiber and is independent of other factors like the wavelength of light and some fiber characteristics.

In various applications of the fiber as a sensor, a helical geometry of the fiber is preferred. In such cases, the geometric rotation of polarization is quite significant; of the order of a few degrees, especially for large pitch helices. In a fiber optic current sensor, the magnetic field due to the electric current in a conductor induces a rotation of the polarization of the light in the fiber due to Faraday rotation.^{16,17)} This rotation is proportional to the current and is a fairly small rotation; comparable to the rotation caused by other birefringence effects discussed in Chapter 2. A slight change in the path of the fiber may cause a large rotation comparable to or greater than the Faraday rotation. It is therefore important to calculate this effect in such applications. The large rotations may also be used advantageously to isolate the Faraday rotation from other stress induced linear birefringence effects discussed earlier.

3.1 PROPAGATION OF POLARIZATION IN A CURVED FIBER

As discussed in Chapter 1, the propagation of light in a fiber is based on the principle of total internal reflections. It was also shown that in the case of a straight fiber, the state of polarization of light is preserved, in the absence of any linear birefringence. This, however, is not obvious in the case of a curved fiber.

When light is internally reflected, the perpendicular and parallel components of the E field undergo different phase shifts, as indicated by fig.2.2. If linearly polarized light is launched inside a straight fiber such that the E field is polarized perpendicular to the waveguide axis, then there is no parallel component of the E field at any time and hence in the absence of any birefringence, the polarization of the linearly polarized light is preserved. However, in the case of a curved fiber, the waveguide axis and hence the propagation direction changes along the curve. Thus at any time, the E field must be resolved into a parallel and perpendicular component, each of which will undergo a different phase shift. This could change the linearly polarized character of light.

For the case of single mode fibers it was shown in chapter 1.2, that to a good approximation, we can assume the fiber to be a weakly guiding fiber, i.e. $n_1 - n_2 \ll 1$, where n_1 and n_2 are the refractive indices of the cladding and the core respectively. For such a fiber, the internal reflection angle of light is always approximately 90° . It can be seen from fig.2.2 that the parallel and perpendicular compone-

nts of the E vector do not have a phase lag with respect to each other. In other words, the polarization state of linearly polarized light will not be affected even for a curved fiber.

If we look at the more accurate description provided by the waveguide theory, rather than the ray picture. We saw in chapter 1.3, that in the weakly guiding fibers, linearly polarized modes are propagated. In the absence of any birefringence, the particular mode propagating in a single mode fiber can not undergo any change. i.e., an ideal single mode fiber will always propagate the same mode.

At this point we introduce an axiom known in literature as the principle of constant azimuth or Ross's axiom¹⁴⁾, which states that for a single mode fiber with no birefringence, the angle that the polarization vector makes with the normal to the plane of curvature at any point on the curved fiber is will remain fixed. The implication of Ross's axiom is illustrated in the following section.

3.2 ORIGIN OF THE GEOMETRIC ROTATION

Consider a low birefringence single mode fiber laid on two plates, which are twisted by an angle θ , as shown in the fig.3.1a. The normals to the planes are indicated by N_a and N_b respectively¹⁵⁾.

If linearly polarized light is coupled into the fiber, then from the principle of constant azimuth discussed earlier, the azimuthal angle, i.e. the angle the electric field vector makes with the normal to the plane on which the fiber is laid, remains constant.

Since there is no reason for light to change its direction of

optical vibration at the interface of the two planes, the azimuthal angles on the two planes are related as follows:

$$\phi_b = \phi_o - \theta \quad (3.1)$$

where ϕ_o is the azimuthal angle of the E- field on the first plane.

Next, consider that such an ideal fiber is fixed on two plates A and B as shown in fig.3.1b. Plate B is rotated around an axis by θ . The input and output ends of the fiber are fixed on the same plane of plate A, as shown in fig.3.1b. Let linearly polarized light be launched into the fiber such that the E field makes an angle ϕ_a with the normal N_a . Then, as above, the azimuthal angle on plate B is given as

$$\phi_b = \phi_o - \theta \quad (3.2)$$

If the polarization azimuth of the returning light from plate B to A is denoted by ϕ_a' , then we have, similar to the transit from A to B,

$$\phi_a' = \phi_b - \theta \quad (3.3)$$

Then, from 3.1 and 3.2 it follows that

$$\phi_a' = \phi_a - 2\theta \quad (3.4)$$

Thus, though both the input and the output ends of the fiber are on the same plane, only the change in the intermediate path of the fiber creates the effect of polarization rotation.

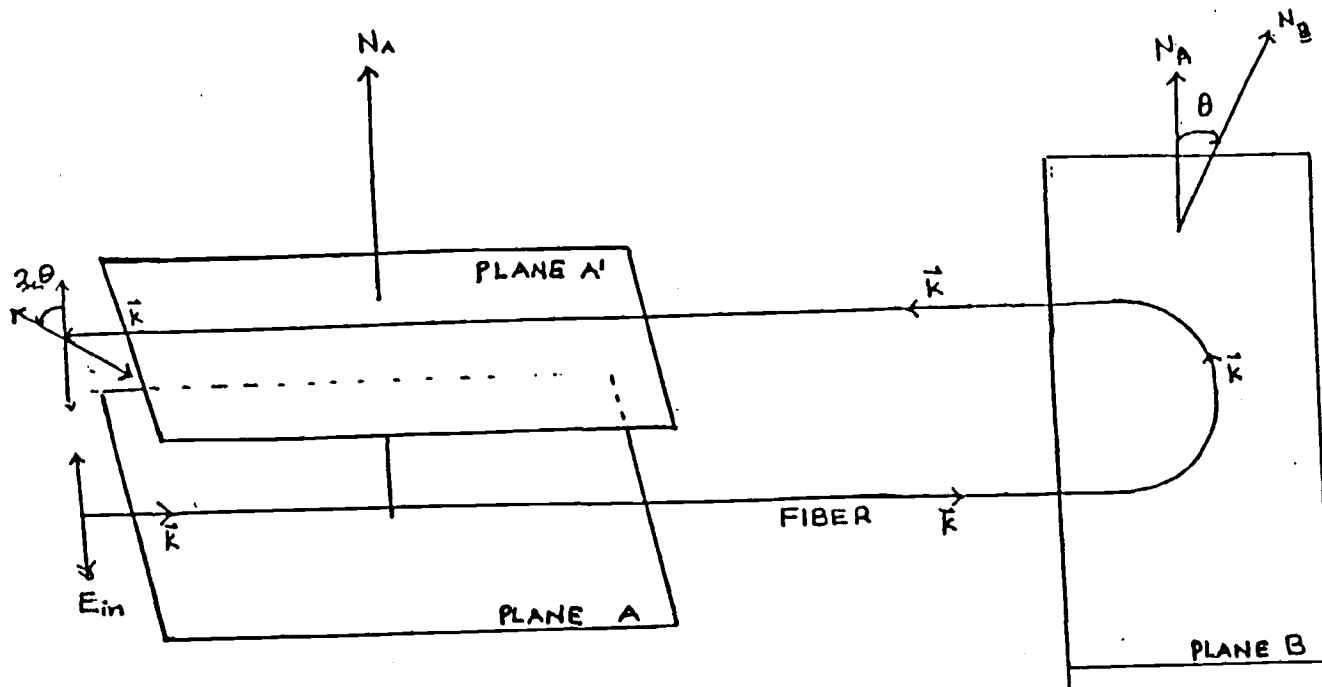


Fig.3.1

Geometric rotation of polarization

3.3 MATHEMATICAL DERIVATION FOR THE GEOMETRIC ROTATION OF A HELICAL FIBER

Now consider a single mode fiber with no intrinsic birefringence. The fiber is assumed to have no other stress induced birefringence effects. Let the fiber axis lie along a non planar curve $r(s)$ where s is the distance along the curved fiber from an arbitrary point P_0 . (fig. 3.2a).

The orientation of the polarization vector is defined with respect to the orthogonal triad of vectors k , n , b as shown in the fig.3.3, where k is the propagation direction tangent to the curve at each point, n is the normal vector, pointing towards the radius of curvature. b is the normal to the plane tangential to the fiber at that point and passing through the the centre of curvature.

Because of the non planar nature of the curve, the vectors b_1 and b_2 at the two points P_1 and P_2 will be at an angle α to each other. Then from Ross's axiom, if the polarization vector makes an angle θ_0 with respect to the normal n_1 , it will have to rotate an angle θ to maintain the same orientation with respect to the normal n_2 . This is illustrated in fig.3.2b.

If the points P_1 and P_2 are close to each other i.e. if ds , the distance along the curve is sufficiently small, then the angle between b_1 and b_2 is defined, from differential geometry, to be

$$\alpha = db/ds = -rds \quad (3.4)$$

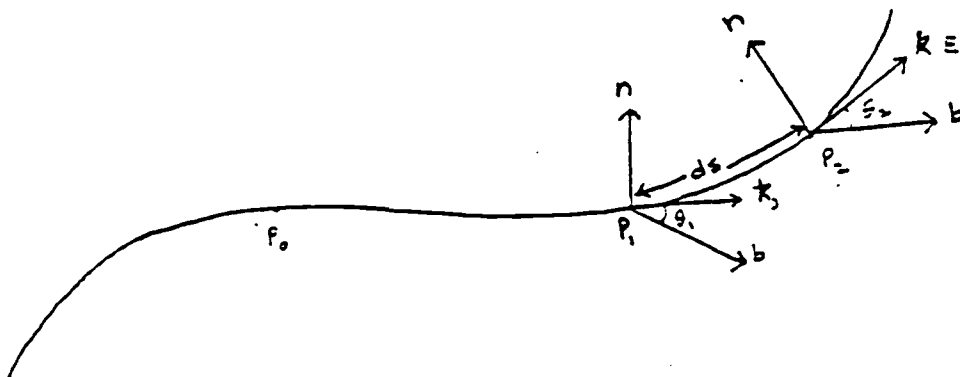
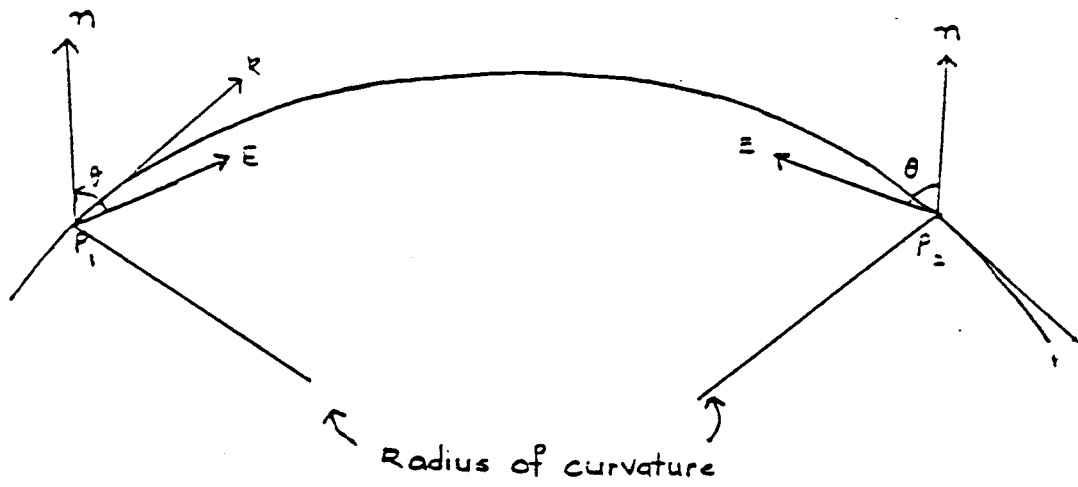


Fig. 3.2.

Axes used to describe the polarization state in a fiber.

$$\text{where } \tau = (2\pi\rho)/((2\pi a)^2 + (p/2)^2) \quad (3.5)$$

for a uniform helix of pitch p and radius a .

Thus in general, the orientation of polarization at a point P with respect to the local normal vector is related to the polarization orientation θ_0 at P_0 by

$$\theta = \theta_0 - \int \tau ds \quad (3.6)$$

Note that if the curve is planar then $\tau=0$ ($p=0$), so that $\theta=\theta_0$ as required. For the case of a uniform helix, the fiber length s of a helix of pitch p and radius a is given as

$$s = 2\pi(a^2 + p^2)^{1/2} \quad (3.7)$$

So, the angle of rotation for a complete helix is given using 1-3 as:

$$\theta - \theta_0 = - \int \tau ds = - 2\pi(p/s) \quad (3.8)$$

Note that the rotation depends only on the pitch and the length of the helical fiber.

This is found to agree with the experimental rotation measured for fibers with different helical geometries. The experiment is discussed in Chapter 5.

CHAPTER 4

BERRY'S TOPOLOGICAL PHASE

The topological phase observed in the helical fiber has received a lot of attention in recent physics literature as a manifestation of what is now known as Berry's Phase or the Quantum Adiabatic Phase^{19,20}). The angle of rotation is then a measure of the Berry's phase for the photons travelling in the helical fiber. The rotation predicted by this phenomenon agrees with the classical result discussed earlier and with the experimental results²²).

The universality of the phase has stimulated a great deal of interest in physics because it seems to span phenomena as diverse as atomic physics and classical electromagnetism to modern particle physics. This phase factor arises from the adiabatic transport of a system around a closed path in an abstract coordinate system called the Parameter Space. Such a space describes the variation of the various parameters on which the Hamiltonian depends. For example, if we have a Hamiltonian with a changing magnetic field then the parameter space here is the space representing the magnetic field. In the case of the photon propagating in an optical fiber, the direction of propagation is changed, so that the parameter space is the \bar{k} -space.

The most notable feature of this phase factor is its path dependence. The phase carries information about where the system has been.

It thus stores the memory of the past.

The origin of this phase can be explained very elegantly by simple "topological experiment" described here.

Consider a pointer held tangentially on the surface of a globe so that it is on the equator and parallel to it. Keeping the pointer tangential to the surface at all times, take it on a closed circuit around the globe so that it is always parallel to its original direction. Move it around the equator 90° and then move it toward North Pole along a longitudinal line. Upon reaching the North Pole, move it back down the longitude that intersects the starting point. At the end of the circuit, the pointer will have rotated 90° .

The rotation occurs despite the best efforts to maintain the pointer in a fixed orientation with respect to the local environment. This is because of the curvature of the sphere. Note that it is crucial to go around one of the poles to get the rotation. In mathematics, such a phenomenon is known as the parallel transport of vectors.

The curvature of the earth's surface is related to the curvature of the parameter space. It is this curved surface which gives rise to the topological phase. Different paths on the parameter space correspond to different phases.

4.1 GENERAL DERIVATION OF BERRY'S PHASE

The adiabatic evolution of a Quantum mechanical system is described by the Quantum Adiabatic Theorem which states that when stationary

state of a quantum mechanical system undergoes an adiabatic cyclic evolution then at the end of the cycle the wave function is modified only by a dynamical phase factor $\exp(-iEt/\hbar)$.

The British physicist Michael Berry modified the theorem by predicting an additional phase factor which depends on the path of evolution and is known as Berry's phase or the Quantum Adiabatic Phase.

To derive a general expression for this phase let us consider a physical system described by a Hamiltonian $H(\vec{R})$ where $\vec{R} = (\vec{R}_1, \dots)$ corresponds to the different parameters on which the Hamiltonian depends. For example, \vec{R} could correspond to different components of the magnetic field for a system of an electron in a changing magnetic field.

Let the system be in a stationary state. From the time dependent Schrödinger equation, the time evolution of the state is given by:

$$H(\vec{R}(t))|\psi(t)\rangle = i\hbar\partial/\partial t|\psi(t)\rangle \quad (4.1)$$

Taking Berry's prediction as an *Ansatz*, we have from the modified Adiabatic Theorem,

$$|\psi(t)\rangle = \exp(-iEt/\hbar)\exp(i\gamma_n(t))|n(\vec{R}(t))\rangle \quad (4.2)$$

where $\gamma_n(C)$ is Berry's phase.

Substituting 4.2 into 4.1 we get,

$$-i\gamma_n(t)|n(\vec{R}(t))\rangle = |\nabla_{\vec{R}}n(\vec{R}(t))\rangle \cdot \vec{R}(t) \quad (4.3)$$

so, the total phase change around C is given by:

$$\gamma_n(C) = i \oint \langle n(R) | \nabla_{\vec{R}} n(\vec{R}) \rangle d\vec{R} \quad (4.4)$$

Apply Stoke's Theorem to 4.4, then

$$\gamma_n(C) = i \iint \nabla \times \langle n(\vec{R}) | \nabla_{\vec{R}} n(\vec{R}) \rangle \cdot d\vec{S} \quad (4.5)$$

Let us denote $V_n(\vec{R})$ as

$$V_n(\vec{R}) = \nabla \times \langle n(\vec{R}) | \nabla_{\vec{R}} n(\vec{R}) \rangle = \langle \nabla n | \times | \nabla n \rangle \quad (4.6)$$

Now, for any eigenstate $|n\rangle$ of the Hamiltonian,

$$H|n\rangle = E_n|n\rangle \quad (4.7)$$

Using completeness, we can write 4.6 as:

$$\begin{aligned} V_n(R) &= \sum_{m \neq n} \langle \nabla n | m \rangle \times \langle m | \nabla n \rangle \\ &= \sum_{m \neq n} \langle \nabla n | m \rangle \times \langle m | \nabla n \rangle + \langle \nabla n | n \rangle \times \langle n | \nabla n \rangle \end{aligned} \quad (4.8)$$

From normalization we know,

$$\langle n | n \rangle = 1$$

$$\text{so, } \langle \nabla n | n \rangle + \langle n | \nabla n \rangle = 0$$

$$\text{i.e. } \langle \nabla n | n \rangle = -\langle n | \nabla n \rangle$$

$$\text{so } \langle \nabla n | n \rangle \times \langle n | \nabla n \rangle = 0$$

Also,

$$H|n\rangle = E_n|n\rangle$$

so,

$$dH|n\rangle + H|dn\rangle = E|dn\rangle$$

$$\Rightarrow \langle m | \nabla n \rangle = \langle m | dH | n \rangle / (E_n - E_m) \quad (4.9)$$

Substituting in 4.8, we get

$$V_n(R) = \sum_{m \neq n} \frac{\langle n | \nabla_R H | m \rangle \langle m | \nabla_R H | n \rangle}{(E_m - E_n)^2} \quad (4.10)$$

So, the general expression for Berry's phase is

$$\gamma_n(C) = -i \iint_C d\vec{s} \cdot \vec{V}_n(\vec{R}) \quad (4.11)$$

where V_n is given by eqn.4.10

4.2 PROPERTIES AND SIGNIFICANCE OF BERRY'S PHASE

The general expression for the phase can give some insight into some properties of this phase. We note, from eqn.4.6 in section 4.1, that the expression involves an integrand which is the curl of a vector. i.e.

$$\begin{aligned} \gamma_n(C) &= i \iint_C \nabla \times \langle n(R) | \nabla_R n(R) \rangle \cdot d\vec{s} \\ &= i \iint_C \nabla \times \vec{A} \cdot d\vec{s} \end{aligned}$$

$$\text{where } \vec{A} = \langle n(R) | \nabla_R n(R) \rangle$$

This makes the phase gauge invariant so that it is unaffected by choices of phases of wavefunction. So, if

$$|n(R)\rangle \rightarrow \exp(i\theta(R)) |n(R)\rangle$$

Then,

$$\vec{A}_n(R) \rightarrow \vec{A}_n(R) - \nabla \theta(R)$$

So that γ_n is not affected, since $\nabla \times \nabla \theta(R) = 0$.

The gauge invariance property of Berry's phase brings about the analogy to the vector potential of electromagnetic theory and the Aharonov Bohm

effect, which describes the effect of a vector potential corresponding to zero field. The Dirac phase factor which multiplies the wave function in this effect, has been explained as a special case of the Aharonov Bohm effect. In other words, Berry's Phase has been described as a generalized Aharonov Bohm Effect.

The gauge invariance of Berry's phase has also been an attractive feature to study for theorists. The gauge fields that permeate modern particle physics also have a strong geometrical character. A connection has been made in the recent theoretical physics literature between Berry's phase and such gauge fields^{19,24,31}).

Another consideration of Berry's phase comes about in the Born-Oppenheimer approximation in molecular physics. This relates to the adiabatic excursion of electrons in a rotating molecule. It was shown, that if the internuclear coordinates traverse a circuit within which the state is degenerate with respect to another, then the electronic wavefunction acquires an additional phase of 180° . i.e. it changes sign. This sign change can now be explained as a special case of Berry's phase²⁵).

As we have seen earlier the geometric phase arises from rather general considerations and is thus relevant to many areas of quantum physics³²⁻³⁴).

Condensed matter applications have been found in the statistics pertaining to the fractional quantization of Hall effect. Wilzeck and Zee have presented a generalization of this phenomena to degenerate subspaces, to show how altered quantization conditions arise in simple adiabatic systems^{28,29}).

While these topics are not a subject of our discussion here, they highlight the relevance and significance of this phenomena to different fields in physics.

4.3. MANIFESTATION OF BERRY'S PHASE IN PHYSICAL SYSTEMS

4.3.1. PARTICLE IN A MAGNETIC FIELD

The interaction of a spin s particle with a magnetic field is described by a Hamiltonian^{19,23)}

$$H(\vec{B}) = k\hbar \vec{B} \cdot \vec{S} \quad (4.11)$$

where k is a constant involving the gyromagnetic ratio

and S is the spin operator with $2s+1$ eigenvalues n with integer spacing and that lie between $-s$ and $+s$. The eigenvalues of the Hamiltonian are:

$$E_n(B) = k\hbar Bn \quad (4.12)$$

Here B corresponds to the parameter R in our general analysis.

Since S is in the direction along B , as B is slowly varied, S is rotated in a circuit. This circuit gives rise to Berry's phase factor given by

$$\gamma_n(C) = \int d\vec{S} \cdot \vec{V}_n(\vec{B}) \quad (4.13)$$

where $V_n(B) = \sum_{m \neq n} \langle n | \nabla_B | m \rangle \langle m | \nabla_B | n \rangle / (E_m - E_n)^2$

$$= \sum_{m \neq n} \langle n | \Sigma | m \rangle \langle m | S | n \rangle / (m-n)^2 \quad (4.14)$$

Let us rotate the axes so that the Z -axis is along the direction of B , then

$$(S_x + iS_y) |n, s\rangle = [s(s+1) - n(n+1)]^{1/2} |n+1, s\rangle \quad (4.15)$$

$$S_z |n, s\rangle = n |n, s\rangle$$

From the orthogonality of eigenstates, only the states with $m = n \pm 1$ are coupled with $|n\rangle$ in 4.14.

Making use of 4.15 in 4.14, we get

$$V_n = 1/B^2 \cdot \{ \langle n | S_x | n+1 \rangle \langle n+1 | S_y | n \rangle - \langle n | S_y | n+1 \rangle \langle n+1 | S_x | n \rangle + \langle n | S_x | n-1 \rangle \langle n-1 | S_y | n \rangle - \langle n | S_y | n-1 \rangle \langle n-1 | S_x | n \rangle \}$$

i.e. $V_n(B) = -n/B^2$ (4.16)

Since the expressions $x.V_n(B)$ and $y.V_n(B)$ vanish, therefore

$$V_n(\vec{B}) = -n\vec{B}/B^3 \quad (4.17)$$

and consequently,

$$\gamma_n(C) = - \iint \vec{B} \cdot d\vec{s} / B^3 \quad (4.18)$$

But this is the solid angle Ω that the closed circuit C subtends at $B=0$. So, from 4.16, we have the geometrical phase factor as

$$\exp(i\gamma_n(C)) = \exp(-in\Omega(C))$$

4.3.2 PHOTON IN A HELICAL FIBER

The photon is a massless spin-1 boson. A photon propagating along a direction K can be described by its helicity defined as $S.K$ where s is the spin of the photon. If we denote the photon state as $|k(t)\rangle$ then it always satisfies²³⁾

$$\hat{S} \cdot \vec{K} |k(t)\rangle = |k(t)\rangle$$

Here t represents the optical path and is the helicity quantum number. The helicity of a photon is always ± 1 . For an adiabatic propagation,

the helicity of the photon is invariant so that the helicity quantum number is conserved.

Consider light propagating inside a helical single mode fiber. As it propagates smoothly down the helical waveguide, K is constrained to remain parallel to the local axis of this waveguide, since the momentum of the photon is along this direction. Since its helicity is adiabatically conserved, S is also constrained to remain parallel to the local axis of the waveguide. Thus as the photons propagate down the waveguide the photon spin traces a loop in the parameter space (K_x, K_y, K_z) . Then following the discussion in the previous section, the geometric phase of the photon is given by

$$\gamma_n(C) = \pm \Omega(C)$$

where $\Omega(C)$ is the solid angle subtended by the loop C with respect to $k=0$, i.e. the solid angle subtended by the closed path of K in K space.

In the case of a uniform helix, this is C is a circle so that:

$$\Omega(C) = 2\pi(1 - \cos\theta)$$

Now, how would this phase be detected in this case?

Consider linearly polarised laser light be launched into the fiber.

Then the initial state may be represented as:

$$|X\rangle = 1/\sqrt{2} (|+\rangle + |-\rangle)$$

where, $|\pm\rangle$ are the eigenstates corresponding to $\sigma = \pm 1$. After propagation through the fiber the final state of the photon acquires

the geometrical phase, so that

$$|X'\rangle = 1/\sqrt{2} (|+\rangle \exp(i\gamma_n) + \exp(-i\gamma_n) |-\rangle)$$

Therefore,

$$|\langle X|X'\rangle|^2 = \cos^2 \gamma.$$

By Malus's law, this implies that the plane of polarisation has rotated by an angle which is equal to γ .

Thus the rotation of polarisation observed in a helical fiber can be understood as a manifestation of Berry's phase.

An experiment to verify this phenomenon will be discussed in Chapter 5.

CHAPTER 5

AN EXPERIMENT TO MEASURE THE TOPOLOGICAL
ROTATION OF POLARISATION IN A LOW BIREFRINGENCE
SINGLE MODE OPTICAL FIBER

The objective of the experiment was to measure the rotation of polarization of a low birefringence, single mode fiber following a non-planar path and to verify the manifestation of Berry's topological phase for photons propagating in such a fiber.

Helices with different harmonics of deformation were used as the non-planar path of the fiber. Special care was taken to avoid other birefringence effects caused by twisting and bending the fiber. An analysis of birefringence induced by the stress due to bends and twists was also done.

A computer controlled system to measure the rotation of polarization was designed for the experiment. Within experimental errors, the results of the experiment were found to be in good agreement with the theoretical calculations.

5.1.1 EXPERIMENTAL SETUP

The experimental setup is shown schematically in fig.5.1(a).

The setup consisted of a 5 mw, 633nm He Ne laser, a single mode fiber and a hollow cylinder. The optical fiber was inserted in a loose rubber tube and then wrapped around the cylinder in a helical

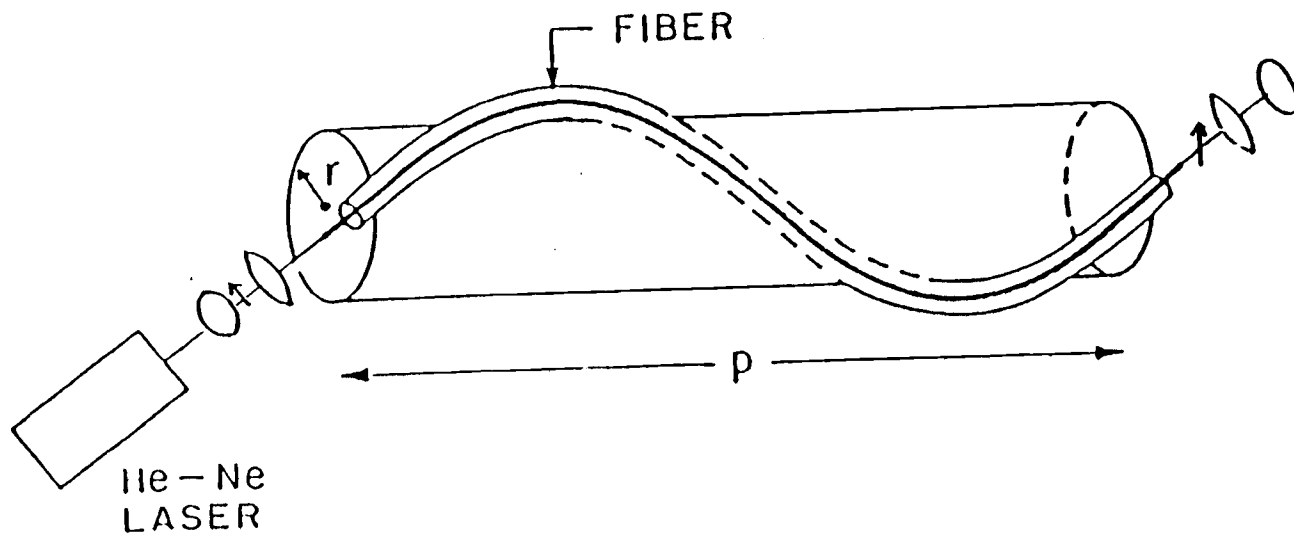


Fig. 5.1. Schematic of the experimental setup.

path. The rubber tube ensured that the fiber was free from torsion.

At the input, the fiber was firmly held by placing the loose tip of the fiber on a groove carved on a piece of cork and fixed on a stand on an optical bench. This held the fiber firmly in place while introducing negligible amount of stress birefringence at the ends. The rest of the fiber, which was in the rubber tube, was relatively free from torsion as it was allowed to move freely within the tube and was also free from any friction introduced while bending the fiber on the cylinder.

The cylinder was clamped on holders on the same optical bench. This ensured the stability of the system. The input and output ends of the fiber were made exactly parallel to each other by placing the ends on stands of exactly the same height and by placing the fiber ends parallel to the optical bench. The propagation directions at the input and output were thus in the same plane and parallel to each other.

5.1.2 SPECIFICATIONS OF COMPONENTS

LASER: 5 mw He-Ne 633 nm laser

COUPLER: Focusing Lens:30 mm focal length

X-Y fiber holder

FIBER: Newport Single mode, step index fiber (F-SV) with Silica core and cladding

V number: $V = 2.19$ at 633 nm

Numerical Aperture: $NA = 0.11$

The output of the He-Ne laser was linearly polarized. The polarization was measured by placing a polarizer analyser combination at the input end. With the direction of polarization along the Y axis, the light was launched into the fiber by a focusing lens and a x-y holder.

A 30 mm lens was used to focus and collimate the beam. To get a good coupling, the fiber tip had to be stripped of the cladding, so that light would be coupled into the core rather than the cladding. This was done by dissolving the cladding at the tip in methylene chloride solution. Stripped of the cladding, it was easy to couple light into the core of the fiber.

A flat end face without any cracks or defects was also required for obtaining good coupling. This was achieved by cleaving the fiber tip with a sharp razor blade or a special fiber cleaver. The small nick from the sharp cutter propagates through the fiber without introducing cracks or defects in the fiber. This was necessary in order to get the correct beam shape and good coupling.

The other factor that affected the coupling was the alignment of the fiber with the focused laser beam. As discussed in Chapter 1, the angle of the incident beam has to be within the numerical aperture of the fiber. Also, the electromagnetic field distribution of the laser beam has to match the profile of the mode propagated by the fiber. A single mode fiber propagates the HE_{11} mode. For a graded index fiber, this is approximated to be a Gaussian distribution:

$$w_0 = a[0.65 + 1.619V^{-1.5} + 2.879V^{-6}]$$

where a is the core radius

w_0 is the radius of the $1/e^2$ intensity point of the beam.

This was calculated to be 2.3 mm.

The spot size of a focusing lens is given by:

$$w_f = f\lambda/\pi w_{in}$$

For our lens, this was found to be 3mm., which was too large to attain optimum coupling. The coupling efficiency, i.e. the ratio of the input light intensity to the output intensity was found to be approximately 30%.

5.1.3 DETECTION AND DATA ACQUISITION

The polarization axis of the linearly polarized light launched into the fiber was aligned at 90° of the polarizer at the input. Thus the minimum of the input intensity was at the 0° position of the analyzer. The light coming out of the fiber was passed through a rotating polariser. The changing intensity of the output light was measured by a negative biased photodiode.

The electrical signal from the photodiode was suitably amplified and then sent to a computer through an 8-bit analog to digital converter. The digitized signal was stored in an IBM-PC/AT. The varying light intensity was thus recorded by the computer which was

able to plot a graph of the intensity.

It was possible to average out the random fluctuations in the intensity by using signal averaging. The computer drove a stepper motor rotating the polarizer with 720 steps per rotation. Taking 100 readings per step, slow enough to average out the fluctuations, we were able to get a smooth sine-wave. The resolution of the graph was $1/2^\circ$. The minimum or maximum intensity points on the graph were used to measure the polarization. The polarization rotation could be determined from the shift in the minimum or the maximum of the intensity plot.

A sample plot is shown in fig.5.2.

The angle of rotation for different geometries of the fiber was thus measured with respect to that of the polarisation at the input of the fiber.

The rotation angles were measured with respect to the output polarisation of the straight fiber as the zero reference.

An uncertainty of measurement of about 3° , was estimated in the data analysis of section 5.4.

5.2 THEORETICAL CALCULATION OF THE ROTATION

In order to form the nonplanar path of the fiber, a paper with a computer generated curve was wrapped on a cylinder and the fiber was laid on top of this curve. This formed the nonplanar path of the fiber. The curves were uniform helices or helices with one harmonic of

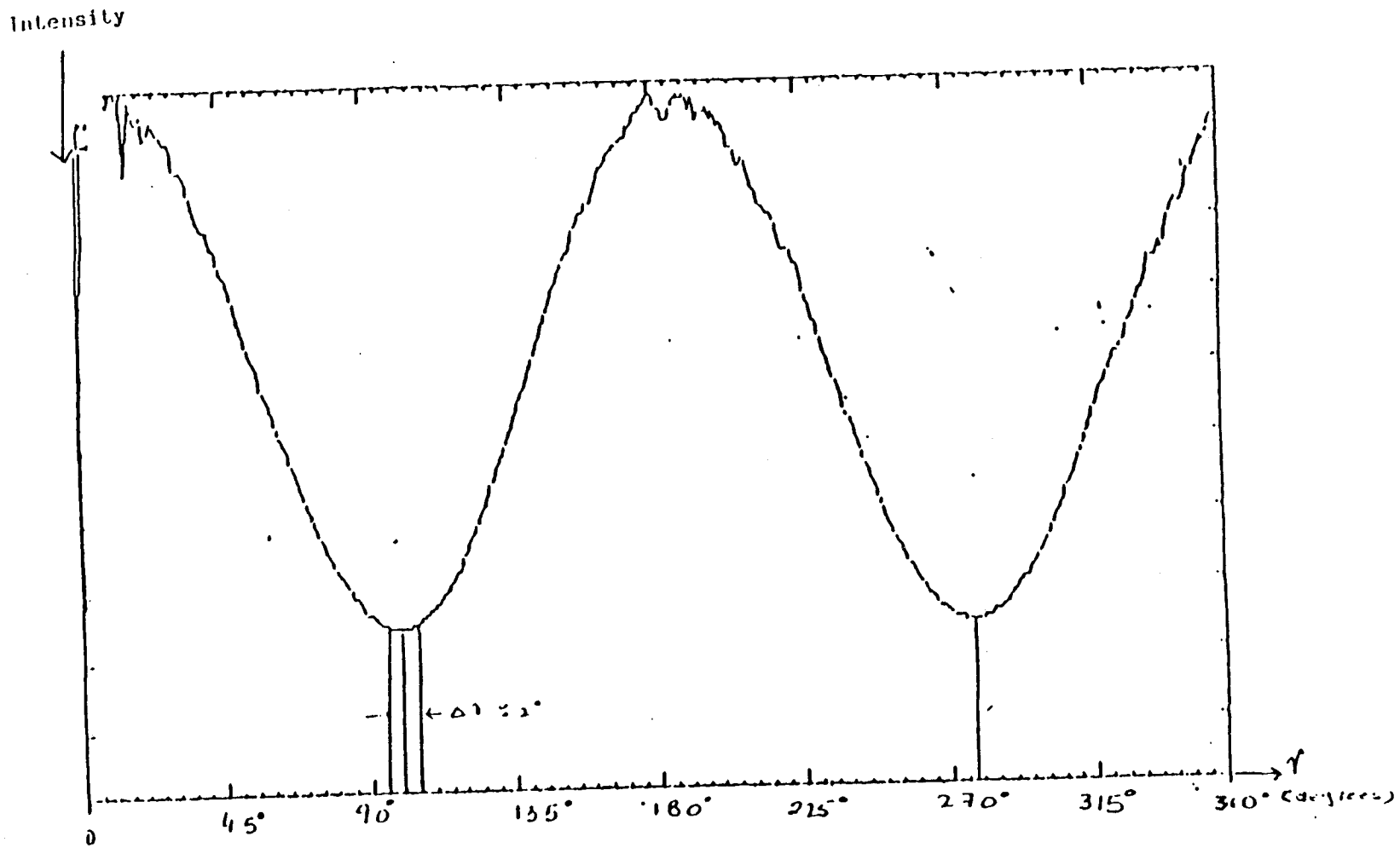


Fig. 5.2(b). A sample intensity plot.

deformation. An example of such a curve is shown in fig.5.3a.

Let the horizontal axis of the paper be the Z axis and the vertical axis be the axis.

Then, using cylindrical co-ordinates, (r, ϕ, z) , the equation of a non uniform helix is:

$$z/r = (p/2\pi r)\phi + A\sin\phi \quad (5.1)$$

where p :pitch of the helix as shown in the figure

r :radius of the helix

A :variable parameter called a harmonic of distortion

$A=0$ corresponds to the case of a uniform helix.

Thus different curves were generated for different values of A on the same cylinder. The experiment was also repeated for two other cylinders with different dimensions.

As can be seen from fig.5.3a, when the curve is unwrapped onto a plane, using cylindrical coordinates (r, ϕ, z) we have

$$\tan \theta(\phi) = (d\phi/dz) \quad (5.2)$$

where $\theta(\phi)$ is the angle between the local waveguide axis and the helix axis as shown in fig.5.3.

Following Berry's theory, this traces out a closed circuit C on the surface of a sphere representing the momentum space. The solid angle in space subtended by C with respect to the centre of the sphere is then given by

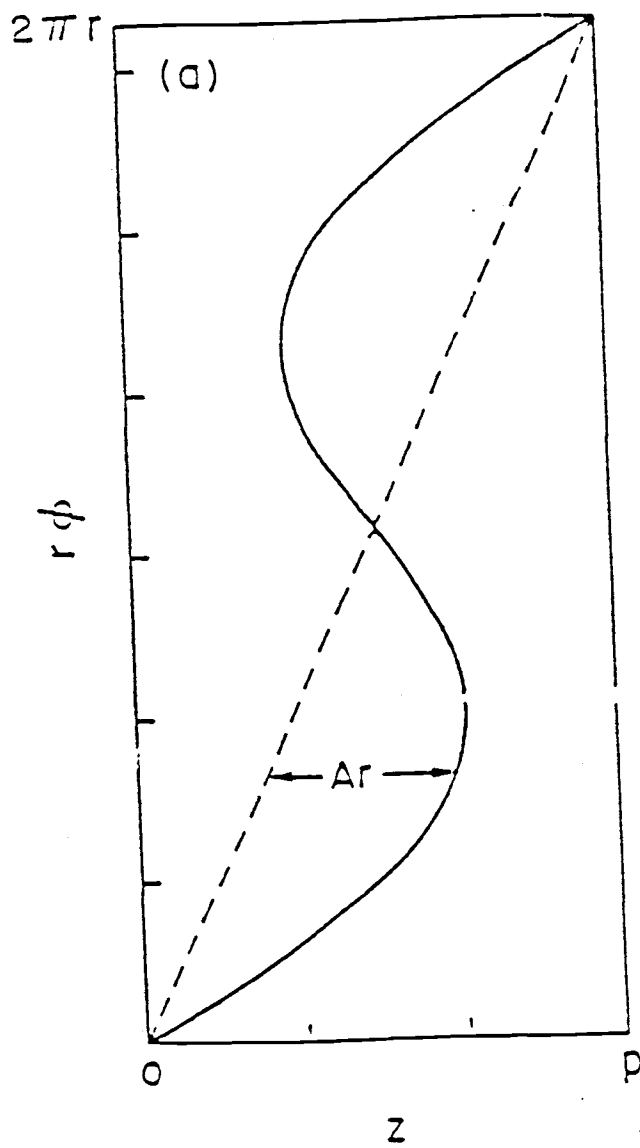


Fig.5.3a Helix geometry.

$$\Omega(C) = \int_0^C \frac{1 - \cos(\theta(\phi))}{s} d\phi \quad (5.3)$$

For the case of the uniform helix, we have, from equations 5.1 and 5.2,

$$\cos(\theta(\phi)) = p/s$$

So that,

$$\Omega(C) = 2\pi(1 - p/s) \quad (5.4)$$

which was the same result derived by using the classical treatment for the case of a uniform helix.

Again from equations 5.1 and 5.2 :

$$\begin{aligned} d\phi/dz &= 1/((p/2) + A\cos\theta(\phi)) \\ \cos(\theta(\phi)) &= (1 + \tan(\theta(\phi)))^{-1/2} \\ \cos(\theta(\phi)) &= \{1 + r[1/((p/2) + A\cos(\phi))]\}^{-1/2} \end{aligned}$$

The integral 5.3 was then evaluated numerically on a computer for different values of A to calculate the corresponding value of the expected rotation.

5.3 DATA ANALYSIS

.....

Theoretical and experimental values of rotation are compared and are found to be in good agreement with each other. Table 5.3 shows the experimental and theoretical values of rotation of polarization for

each cylinder with different harmonics of deformation A. Figures 5.4(a,b,c) show plots of theoretical and experimental values of rotation, in radians, for different helices on cylinders with different dimensions.

The straight line indicates good agreement between theory and experiment.

TABLE 5.3
 MEASURED AND CALCULATED VALUES OF ROTATION FOR
 DIFFERENT CYLINDERS AND DEFORMATIONS
 (IN RADIANS)

A	cylinder 1		cylinder 2		cylinder 3	
	Theory	Experiment	Theory	Experiment	Theory	Experiment
0	0.27	0.31	1.27	1.37	3.45	3.51
0.3	0.25	0.35	1.42	1.54	3.90	3.95
0.6	0.40	0.38	1.83	1.87	4.40	4.38
0.9	0.45	0.43	2.15	2.22	4.45	4.50
1.2	0.62	0.50	3.15	3.10	5.22	5.10

TABLE 5.4
 BEAT LENGTHS OF BEND INDUCED BIREFRINGENCE
 FOR DIFFERENT CYLINDERS

	cylinder 1	cylinder 2	cylinder 3
	$r_1=6.8\text{cm}$	$r_2=10\text{cm}$	$r_2=14\text{cm}$
	$p_1=130\text{cm}$	$p_2=80\text{cm}$	$p_2=43\text{cm}$
Beat length			
(rad/meter)	-0.1	-0.7	-0.17
Fiber length (m)	628	90	37
$2\pi/L_b$ (rad)	0.01	0.06	0.16

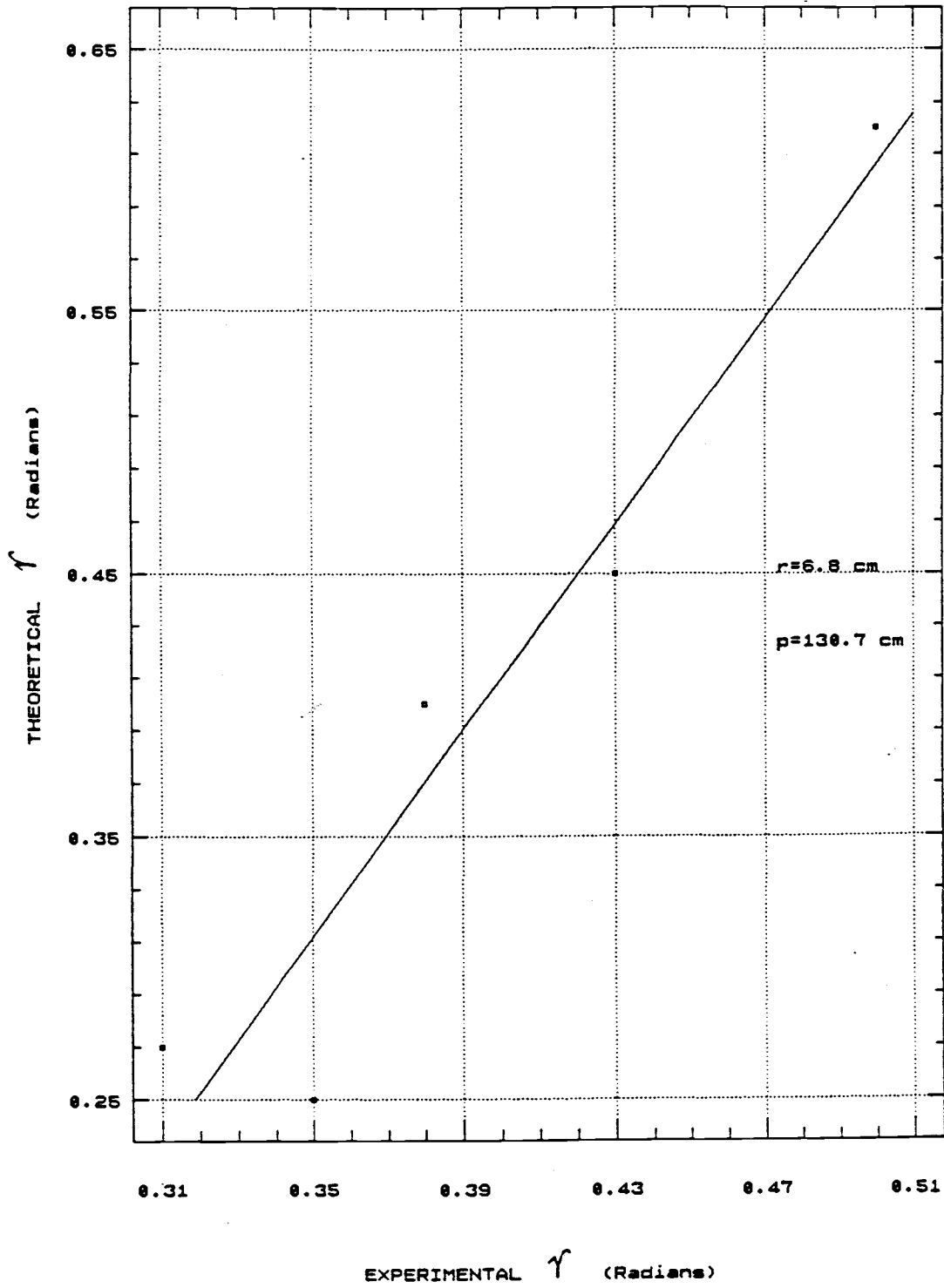


Fig. 5.4(a) Measured rotation of polarization

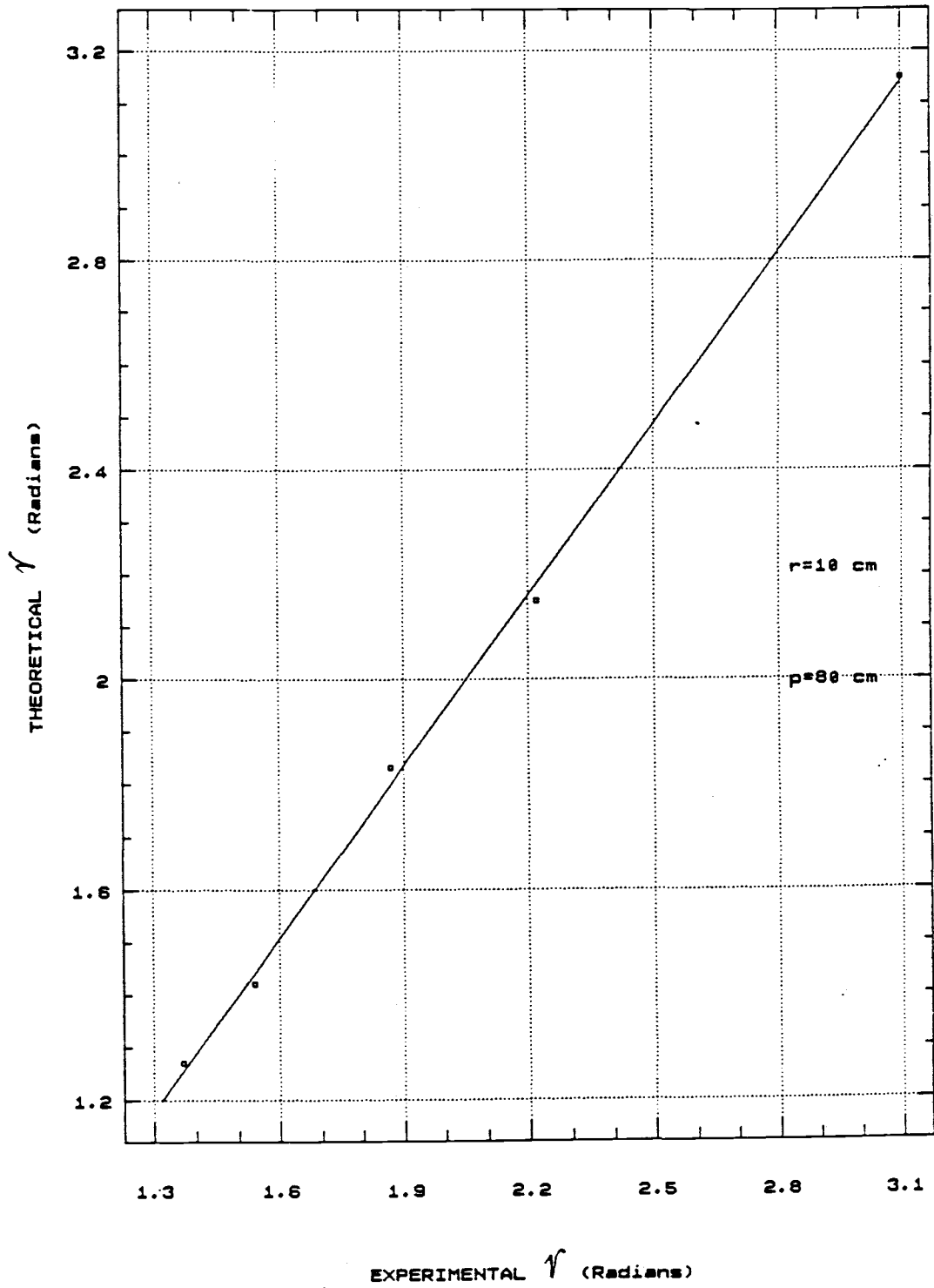


Fig. 5.4(b) Measured rotation of polarization

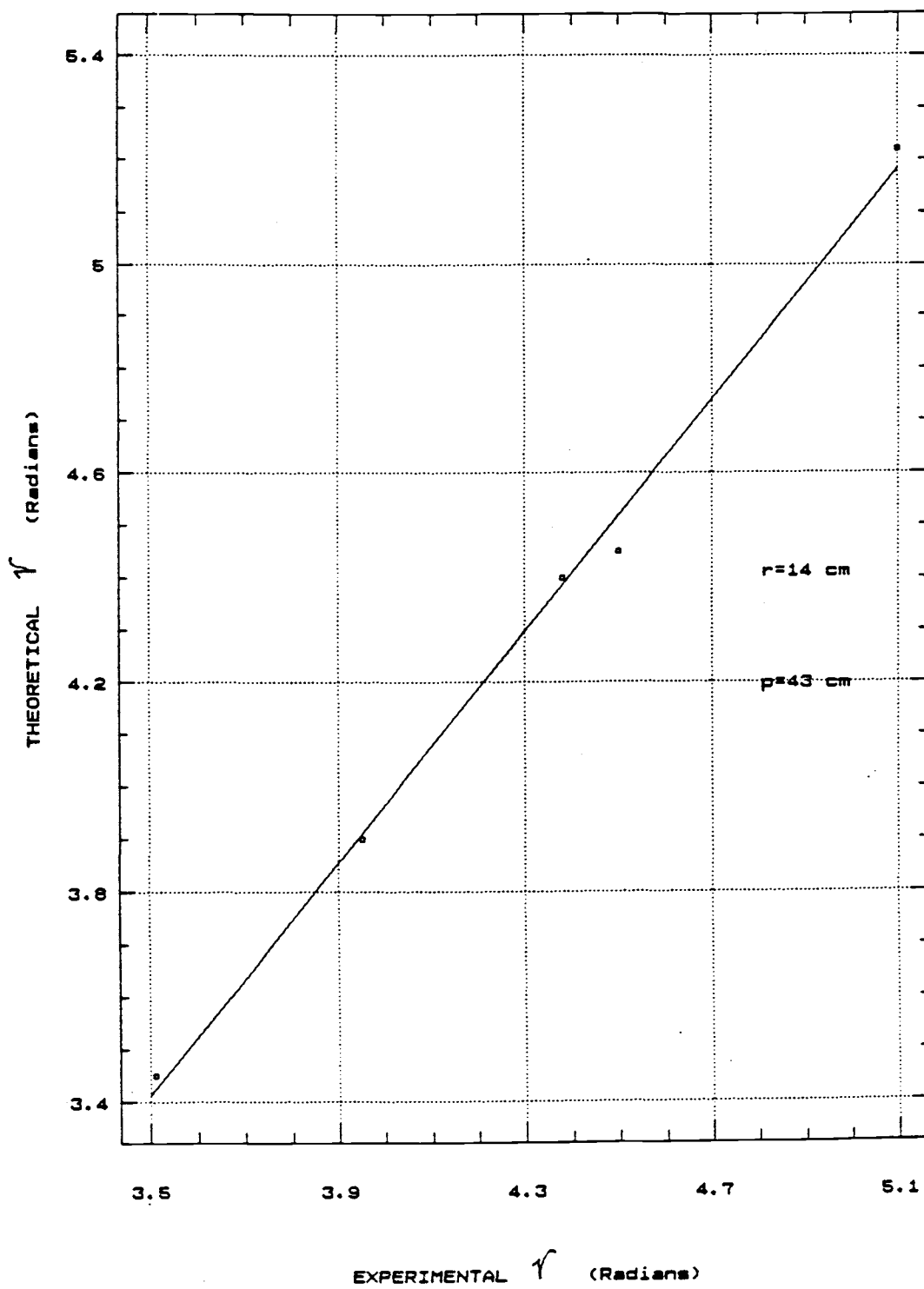


Fig. 5.4(c) Measured rotation of polarization

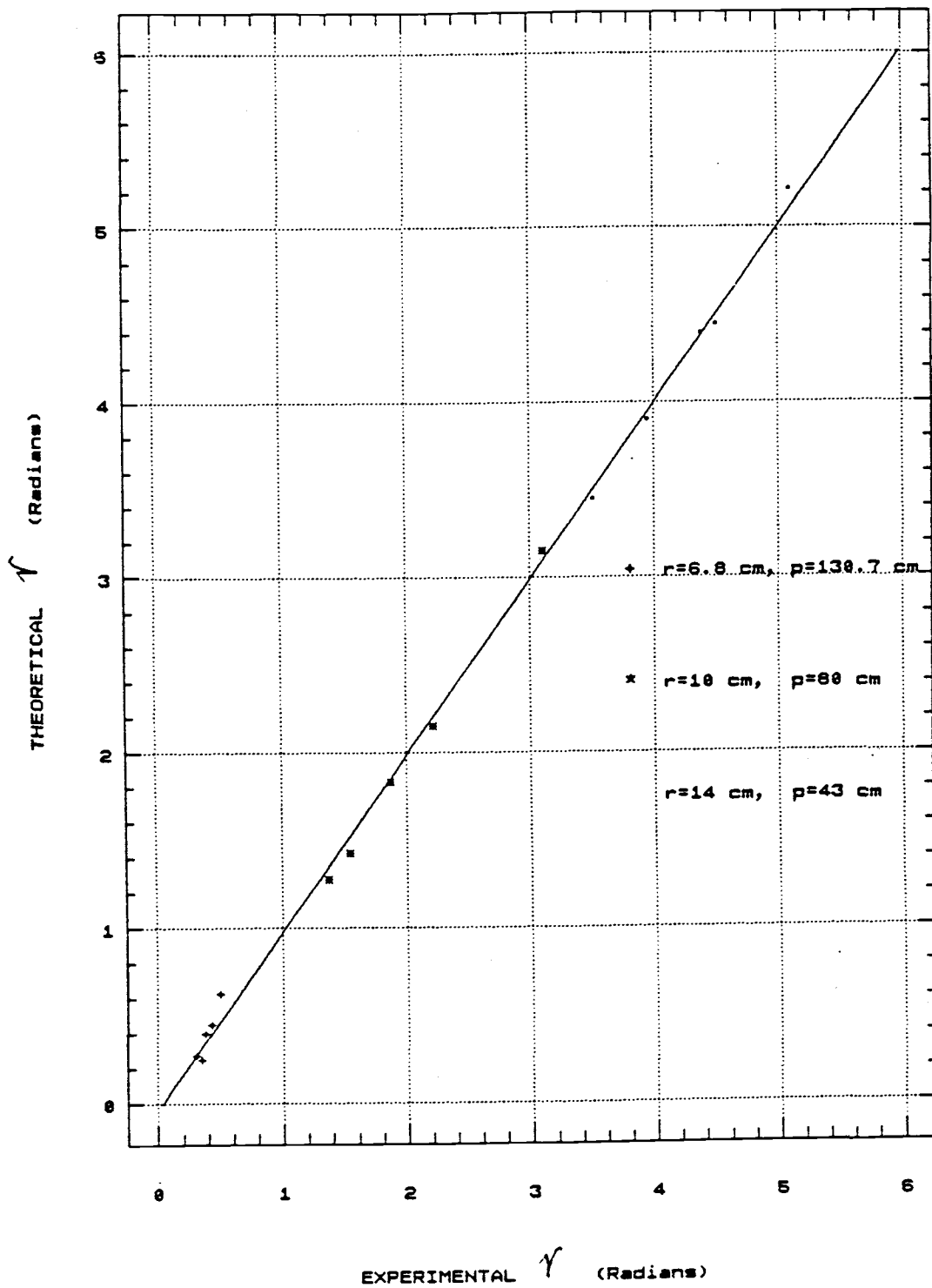


Fig. 5.4(d) Measured rotation of polarization

5.4 ERROR ANALYSIS

The various possible experimental errors due to other birefringence effects and the measuring systems are analysed in this section.

5.4.1 ROTATION DUE TO OTHER BIREFRINGENCE EFFECTS

The calculations of the rotation were done assuming negligible birefringence due to other effects such as stress, twist, torsional or bend induced birefringence.

The errors due to these effects will be calculated .

1. BEND INDUCED BIREFRINGENCE:

The linear retardation due to bend induced birefringence for a fiber with outer radius r is given by

$$\beta_b = Brk \text{ ----->1}$$

where k is the curvature of the bend

B is constant = 1.7×10^7 deg/m

For a uniform helix of pitch p and radius a is given by:

$$k = a/(a^2+p^2) \text{ ----->2}$$

This, however will not give an exact value of the retardation due to the bend induced birefringence. For an exact calculation, we would

have to consider the coupling between linear retardation and circular birefringence due to geometric rotation. It would be necessary to use Jone's calculus to get an exact value of the bend induced rotation. A good estimation can be obtained by comparing the beat length of the linear birefringence with the length of the fiber. The beat length is given by:

$$L_b = 2\pi/B_b$$

Table 5.4 shows the different beat lengths of the bend induced birefringence for different cylinders and the relative errors.

2. TWIST INDUCED BIREFRINGENCE

The circular birefringence induced by a torsional stress due to twists is given by:

$$\beta_t = g\tau$$

where $g = \text{constant} = 0.16$

$\tau = \text{twist rate (rad/m)}$

for a uniform helix of pitch p and radius r ,

$$\tau = [p/2 + 2(r^2)/p]^{-1}$$

For this value of g , it can be seen that even small twist rates contribute significantly to the rotation of polarization. However, twist can be avoided by guiding the fiber loosely in a rubber tube such that it can detwist easily. This was done by inserting the fiber into a rubber tube. The fiber then had sufficient room to detwist when it was wrapped around the cylinder. Looking at the ease of moving the fiber

in the tube even after wrapping it on the cylinder and the good agreement of the experimental and theoretical values, we can conclude that the tubing reduced this effect considerably.

3. INTRINSIC BIREFRINGENCE

The intrinsic circular and linear birefringence due to anisotropies in the fiber core and other fabrication defects was measured by laying the fiber straight and launching linearly polarized light through it.

We could not measure any rotation of polarization or ellipticity for the straight fiber with the sensitivity of our measuring system. The rotation of polarization caused by these birefringence effects must be less than 0.5, the sensitivity of the measuring system used.

5.4.2 ERRORS DUE TO THE MEASURING SYSTEM

The shift in the positions of the minima of the intensity plot was considered as a measure of the rotation of polarization for different paths of the fiber. The finite width of the minima thus introduced an uncertainty in the measurement which was of the order of 2° .

5.5 EXTENSION OF THE EXPERIMENT TO FARADAY ROTATION:

As discussed in Chapter 2, a magnetic field applied longitudinally along a fiber will induce a circular birefringence through the Faraday

effect. The rotation due to a coil of N turns, carrying a current I per turn, is given as:

$$\theta_f = VNI$$

where V is Verdet's constant = 4.66×10^{-6} rad/amp

The setup to measure the geometric phase can be used to measure Faraday rotation. Since the value of V is of the order of 10^{-6} only, even a fairly large current would result in a relatively small rotation. This is usually comparable to other linear birefringence effects found in the fiber. The circular birefringence effects due to the geometric phase and Faraday rotation together would be large enough to quench other linear birefringence effects.

To measure Faraday rotation, we can wrap a coil of N turns over the helical fiber with N turns. The rotation with and without any current through the coil could be measured using the system described above.

The corresponding intensity plots, when subtracted from each other would yield a value of Faraday rotation to a good approximation. This could form the basis to develop a non contact current measuring optical fiber device.

If a current carrying coil was wound over the helical fiber then the Faraday rotation would add to the geometric rotation of Berry's phase.

The intensity plots with the magnetic field on and off could be subtracted from each other to give a value for the Faraday rotation.

CHAPTER 6

SUMMARY AND CONCLUSIONS

The experiment verified the manifestation of Berry's phase for photons propagating in a helical waveguide. The theoretical and experimental values of rotation of polarization were in good agreement. The errors and uncertainties involved in the experiment were found to be of acceptable magnitude.

It has been debated in recent physics literature, that this does not confirm Berry's phase at the quantum mechanical level, since a laser beam was used in the experiment. This corresponds to an enormous number of photons in a single coherent state, rather than a single photon. The experiment, however, does support the topological feature of classical electromagnetic theory which originates at the quantum level, but survives the correspondence limit into the classical level. In that sense, it is analogous to the Aharonov Bohm effect seen in electromagnetism and is explained at the level of quantum mechanics. It should be noted that Berry's phase for neutrons has recently been verified experimentally.

Berry's phase thus provides a base for an interesting discussion of the correspondence between classical and quantum physics. The derivation of the geometric phase using boundary conditions of electro-

magnetic theory and parallel transport of vectors yields the same result as that predicted by Berry, for the case of a nonuniform helix. It would, however, be a nontrivial problem to derive it for the more general case of, say, a uniform helix.

The experiment also facilitated an interesting study of polarization properties of a helical fiber, which is important in the context of the present fiber technology.

REFERENCES

-
1. K. Jones, 'Introduction To Optical Electronics', (Harper & Row, New York, 1987).
 2. A. Yariv, 'Optical Electronics', (Holt, Rinehart and Winston, New York, 1985).
 3. D. Lee, 'Electromagnetic Principles of Integrated Optics', (John Wiley & sons, 1986).
 4. L. Jeunhomme, 'Single Mode Fiber Optics: Principles and Applications', (Marcel Dekker, New York, 1988).
 5. W. Jones, 'Introduction to Optical Fibers Communication Systems' (Holt, Rinehart and Winston, New York, 1988).
 6. E. Hecht, 'Optics', (Addison-Wesley, Mass., 1987).
 7. R. K. Jones, J. Opt. Soc. Am., 31, 488(1941).
 8. C. Tsao, J. Opt. Soc. Am., 4, No. 8, 1407(1987).
 9. Ohtsuka, Ando, Imai, J. lightwave Technol., LT-5, No. 4, 602(1987)
 10. J. Noda, Okamoto, Sakai, J. lightwave Technol., LT-4, No. 8, 1071 (1986).
 11. Ulrich and Simon, App. Opt., 18, No. 13, 2241(1979).
 12. Shibata, Tsubokawa, Ohshai, Kitamaya, Seikai, J. Opt.Soc. Am. A,
 13. A. Alphones, G. Sanyal, J. Lightwave Technol., LT-5, No. 4, 598(1987).
 14. J. N. Ross, Opt. Quantum Electron., 16, 455(1984).
 15. Itoh, Saitoh, Ohtuska, J. Lightwave Technol., LT-5, No. 7, 916(1987).
 16. Day, Payne, Barlow, Hansen, Opt. Lett., 7, No. 5, 238(1982).
 17. Berwick, Jones, Jackson, Opt. lett., 293, 12, No. 4, 293(1987).
 18. M. Schwartz, S. Green, W. Ruteledge, 'Vector Analysis with Applications to Geometry and Physics', (Harper & Row, New York, 1980).
 19. M. V. Berry, Proc. Roy. Soc. London, Sec. A392, 45, (1984).

20. 'Fundamental Aspects of Quantum Theory', edited by V. Gorini and A. Frigerio, (Plenum, New York, 1986).
21. R. Chiao and Wu, Phys. Rev. Lett., 57, 933(1986).
22. R. Chiao and A. Tomita, Phys. Rev. Lett., 57, 937(1986).
23. A. Messiah, 'Quantum Mechanics', (N. Holland, Amsterdam, 1966).
24. Aharanov and J. Anandan, Phys. Rev. Lett., 58, 1593(1987).
25. Hua-Zhong Li, Phys. Rev. Lett., 58, 539(1987).
26. G. Delacretaz, E. Grant, R. Whetten, Phys. Rev. Lett., 56, 2598(1986).
27. G. W. Semenoff and P. Sodano, Phys. Rev. Lett., 1195(1986).
28. Moody, A. Shapere, F. Wizeck, Phys. Rev. Lett., 56, 893(1986).
29. H. Kuratsuji and S. Ida, Phys. Rev. Lett., 1003, (1986).
30. Haldane and Wu, Phys. Rev. Lett., 55, 2887, (1985).
31. R. Jackiw, Comments on Atomic and Molecular Physics, D 21, 71, (1988).
32. Frank Ham, Phys. Rev. Lett., 58, 725, (1987).
33. J. Hannay, J. Phys. A., 18, 221(1985).
34. T. Bitter, D. Dubbers, Phys. Rev. Lett., 59, 251, (1987).